Summer Student Report

BRIL (Beam, Radiation and Instrumentation Luminosity)

Luminosity measurements at CMS using DT Phase 2 Demonstrator

Luis Andres Chicaiza

luis.chicaiza04@epn.edu.ec

Supervisor: Alexey Shevelev

2023

Abstract

In Phase-2, CMS will rely on multiple detector systems and, in particular, DT Luminosity, this is the Synchronous histogramming of muon trigger primitives. In this phase hits from DT and RPC detectors will be combined to reconstruct muon track segments. The demonstrator system is equipped with 5 back-end boards. This report shows an analysis of several datasets recorded in 2023. Most of the analysis was performed for Fill 9062 (Stable Beams, 2452 colliding bunches). Background contributions such as type1 afterglow hits, cosmic and beam induced were analysed. Finally, the luminosity for one of the boards was computed.

Contents

1 Introduction

The CMS Beam Radiation, Instrumentation and Luminosity (BRIL) group is in charge of the measurement of luminosity, beam conditions and radiation fields at the CMS experiment. The project not only operates and develops new detectors but also techniques for measuring luminosity under phase 2 of the LHC upgrades (also for the high luminosity upgrades at the LHC).

Luminosity is one of the most important performance parameters of an accelerator, this is the reason that a big experiment like CMS has more than four detectors in charge of delivering this kind of measurement. Luminosity is an estimate of the number of particles that can collide inside an accelerator in a given amount of time and therefore, is not exactly a collision rate. However, it can give an understanding of how many events could take place in a particle collider [1].

2 The CMS Drift Tubes

The DT system is located in the barrel of the CMS detector, in a region where $|\eta| < 1.2$ because background levels are low. Each tube is 4cm wide and contains a stretched wire in a gas volume [2]. Then, if a charged particle goes through it ionizes the gas and the resulting electrons get pulled by the field to the positive wire. The time an electron takes to reach the positive wire combined with its position along the wire where it hit, gives two coordinates of the particle's position.

3 Luminosity of colliding beams

It is usually assumed that beam density distributions have Gaussian profiles in all directions. Therefore, in the case of a beam, which is arranged into discrete packets of protons called bunches, it is necessary the introduction of the accelerator orbit frequency f, the number of bunches per beam N_b and the number of particles in the colliding bunches N_1 and N_2. Then, a commonly used expression for luminosity can be derived:

$$\mathcal{L} = \frac{N_1 N_2 N_b f}{4\pi\sigma_x\sigma_y}$$

where σ_x, σ_y are the corresponding beam widths.

Then for the visible cross section:

$$\sigma_{vis} = \frac{R}{\mathcal{L}} = \frac{4\pi R\sigma_x\sigma_y}{N_1N_2N_bf}$$

Finally, it is important to mention that the LHC usually operates with 2452 bunches of protons that circulate in each ring inside the machine. Each bunch is 25 ns apart from each other and each of them contain roughly 100 billion protons.

This means that the time to complete one orbit is

$$1\,\text{orbit} = 3564\ \cdot 25\,\text{ns} = 89\,\mu\text{s}$$

where 3564 is the total number of possible configurations (or number of bcids), both with protons or empty. Then, a lumi nibble (NB) is defined as the time it takes to complete 4096 orbits, so

$$1\,\text{NB} = 4096\,\text{orbits} = 0.36\,\text{s}$$

However, the nibble-4 (NB4) is more commonly used, such that

$$1\,\text{NB4} = 4\text{NB} = 1.4\,\text{s}$$

Finally, a lumi section is defined as

$$1\,\text{LS} = 64\,\text{NB} = 23\,\text{s}$$

and it corresponds to the granularity (that is, the scale or level of detail in a set of data) of the luminosity.

4 Using the rates of muon trigger primitives for measuring luminosity

One of the ways CMS will measure the luminosity during LHC Phase-2 is by using the rates of muon trigger primitives, that is the Drift Tubes (DT) luminometer. The tests that are currently being carried out during RUN 3 are called DT demo.

Figure 4.2 illustrates the mean number of hits (rates) of each bcid recorded by all the channels/boards of the DT system. Normalization to the actual number of aggregated histograms (orbits) was needed. On the

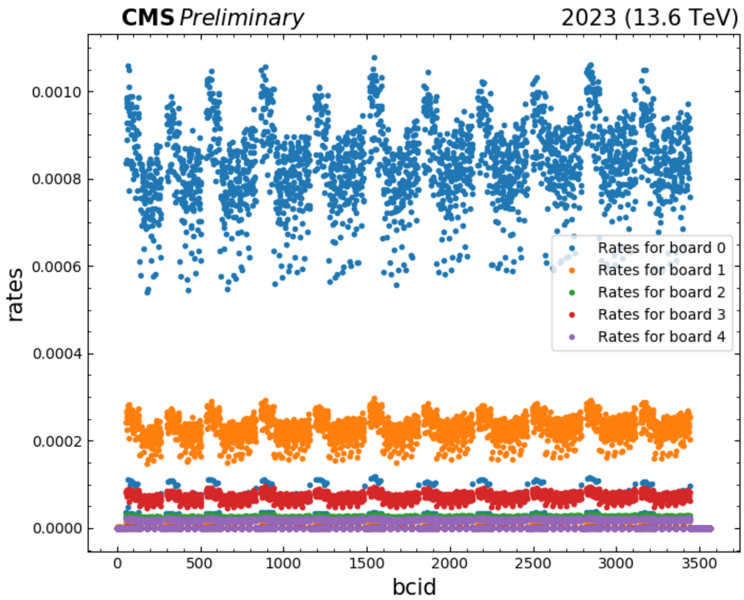

Figure 4.2: Average number of rates for each bcid

other hand, this also shows that the board 0 is able to detect more counts compared to the others. This is related to different location of Front-end modules and corresponding muon fluxes. In particular, board 0 is the closest to beam pipe.

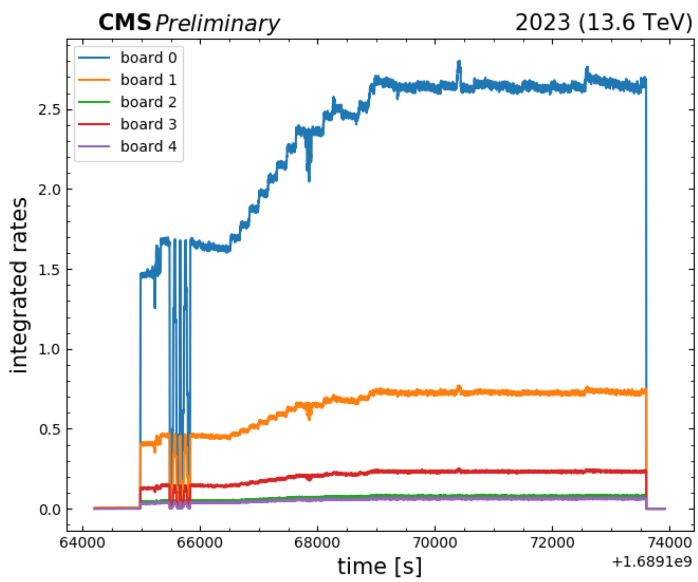

Figure 4.3: Integrated raw rates from DTLumi system (normalized by number of aggregated orbits) during Fill 9062

In Figure 4.3, integrated raw rates (muon trigger primitives) measured by multiple channels of DT Phase 2 demonstrator during stable beams for Fill 9062, are observed. The sum over all 3564 bcid is using a special bunch-mask, this produces orbit integrated rates that can be converted to instantaneous luminosity after proper calibration in emittance scan.

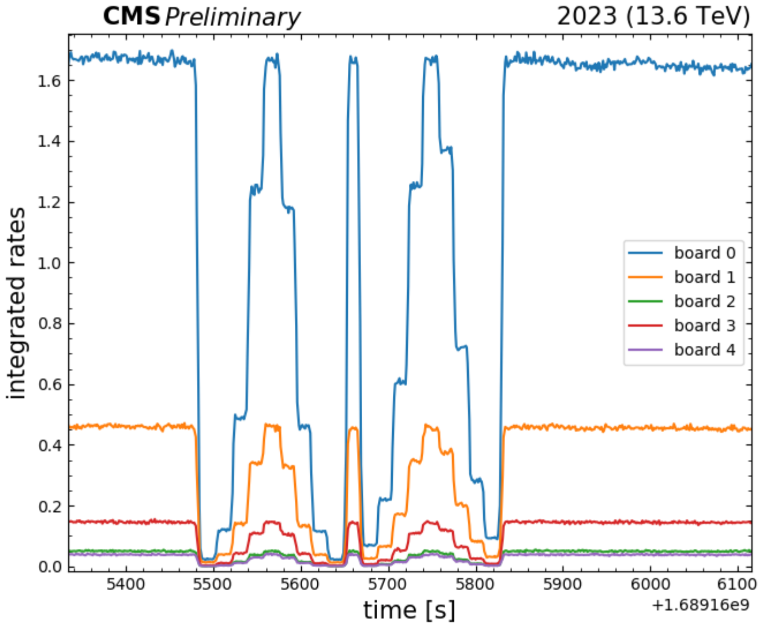

Figure 4.4: Raw rates during emittance scan performed by LHC (Fill 9062)

Figure 4.4 shows integrated raw rates of DT system during an emittance scan which is used to calibrate the detector (to convert raw rates to luminosity $Hz/\mu b$). For example, for board 0, the maximum number of integrated rates, approximately 1.75, is the point when head-on collisions take place. Then, when the beams are separated, because of the emmitance scan, the number of counts decrease almost to zero. After that, the beams are moved to extract the beam shape (profile), which helps us to perform calibrations.

The reason for what the DT system is used, is because muons leave a clean signature, so this could lead to have a more accurate measurement. However, there are also contributions of backgrounds such as out of time collisions (type 1 afterglow hits), cosmic radiation, and beam induced background.

Type 1 Afterglow hits are hits produced in a detector in a bunch crossing after the originating collision, either due to electronic effects in the detector hardware or physical effects in the surrounding material.

5 Results

In order to analyse the Type 1 Afterglow Hits, we have to find colliding bcids before a non-colliding bcid. Then, we find the number of rates of the non-colliding bcid and divide this number to the number of rates of the colliding bcid. In this way, we estimate the fraction of the out of time hits in an colliding bcid. This contribution is called Fraction of Type1 Afterglow Hits.

As we can see in Figure 5.5, we plot the Fraction of Type1 Afterglow Hits as a function of the rates in the colliding bcid.

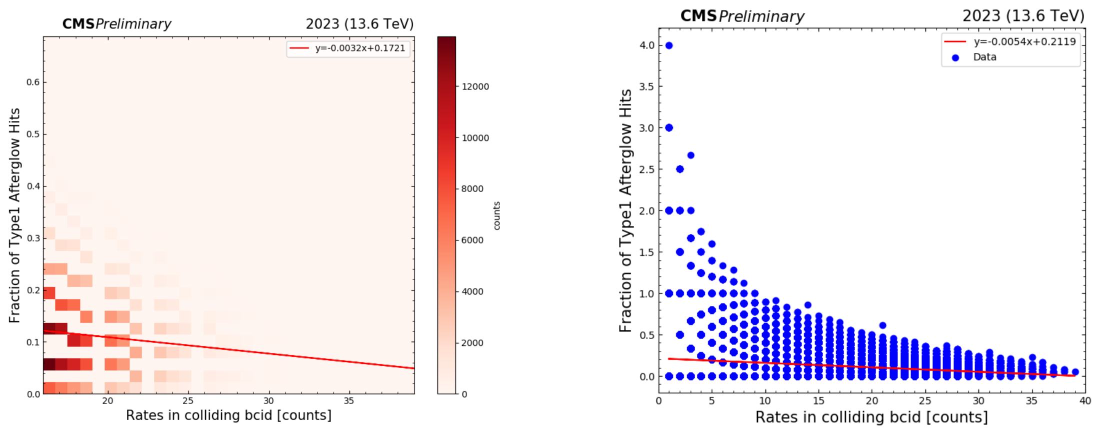

Figure 5.5: Figure (a) is a density plot which shows that for NB4 there are more hits in a low rate region. Figure (b) shows that the data is spread out which means a high uncertainty.

Furthermore, we performed a linear fitting, $y = ax + b$ so that we can estimate the parameter b which can be understood as the percentage of Type 1 hits in a colliding bcid.

For better estimating the Type1 Afterglow fraction we ploted a histogram which can be seen in Figure 5.6. However, as we said earlier, if we use NB4 granularity we have high uncertainty due to unphysical ratios at low counts. For this reason, in order to have better statistics we made

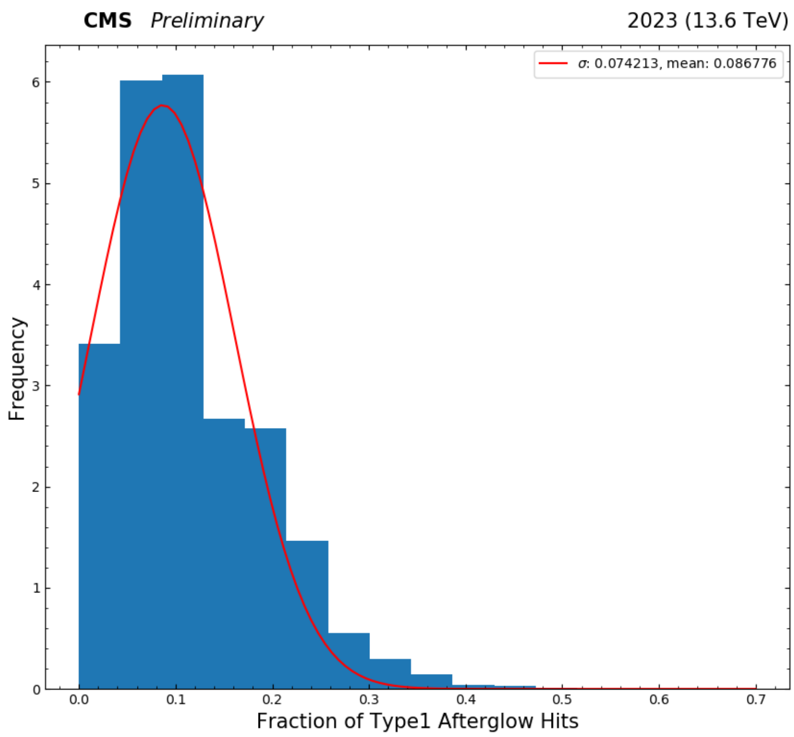

Figure 5.6: Gaussian fitting curve for Type1 Afterglow Hits Fill 9062 (NB4 granularity)

some plots using a lumi section (LS) granularity.

Figure 5.7 shows the fraction of Type1 afterglow Hits as a function of the rates in a colliding bcid using a lumi section granularity. In this plot one can see that the contribution of out of time hits is roughly constant $\approx 13.11\%$. Then to have a better estimation of the contribution of Type1 hits we constructed a fitting curve.

On the other hand, Figure 5.8 shows the parameters that were computed after the fitting. Then, one can notice that the mean value of the Type1 afterglow hits is $\approx 12.72\%$ and this value appears to be approximately constant because the computed slope of the fitting curve is nearly zero. Then, what can also be seen is that the contribution of afterglow hits does not depend on the rates in a colliding bcid.

The mean value of type 1 afterglow hits can be computed for all the channels. The results are show in Table 1.

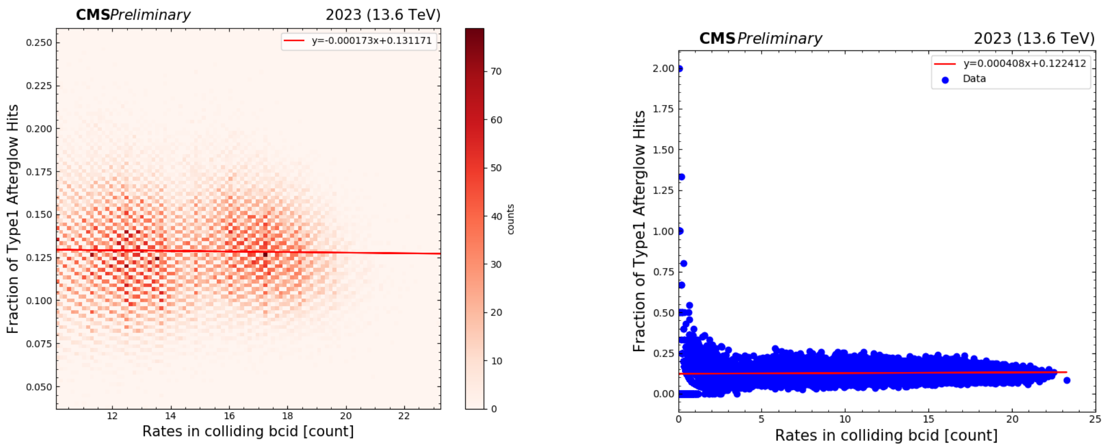

(a) (b)

Figure 5.7: Fraction of Afterglow Hits Vs. Rates in colliding bcid for Fill 9062 (lumi section (LS) sensibility). In figures (a) and (b), it can be seen that the rates are less spread out compared to NB4.

Channel	After glow
0	0.1272
1	0.078
2	0.007
3	0.001
4	0.005

Table 1: Mean values of the contribution of afteglow hits

5.1 Suppressing Type 1 Afterglow Hits

As a next step, we apply the corrections related to type 1 afterglow hits. For this purpose we used the result of the fitting curve showed in Figure 5.8. For example, for channel 0 we have subtracted $\approx 12.72\%$ of the total rates en each colliding bcid. The result can be seen in Figure 5.9.

Figure 5.9 shows the distributions of the integrated rates for channel 0. One can see that the ratio (colliding/non-colliding) increased after corrections. This is a consequence of suppressing type 1 afterglow hits.

Furthermore, the same correction can be applied to every channel. The results for type 1 afterglow hits corrections for channel 1 are shown in Figure 5.10.

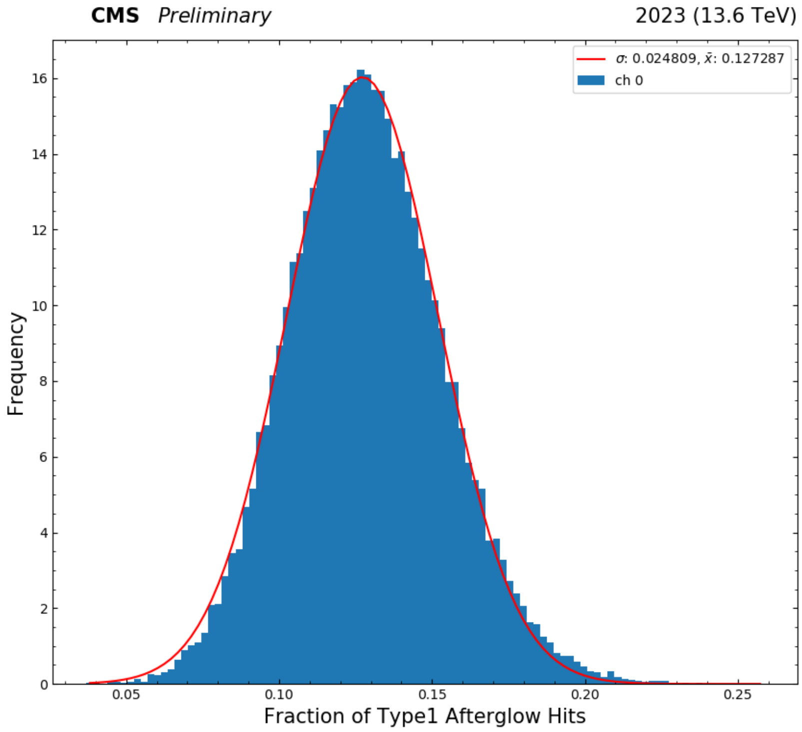

Figure 5.8: Gaussian fitting curve for Type1 Afterglow Hits Fill 9062 (lumi section sensibility)

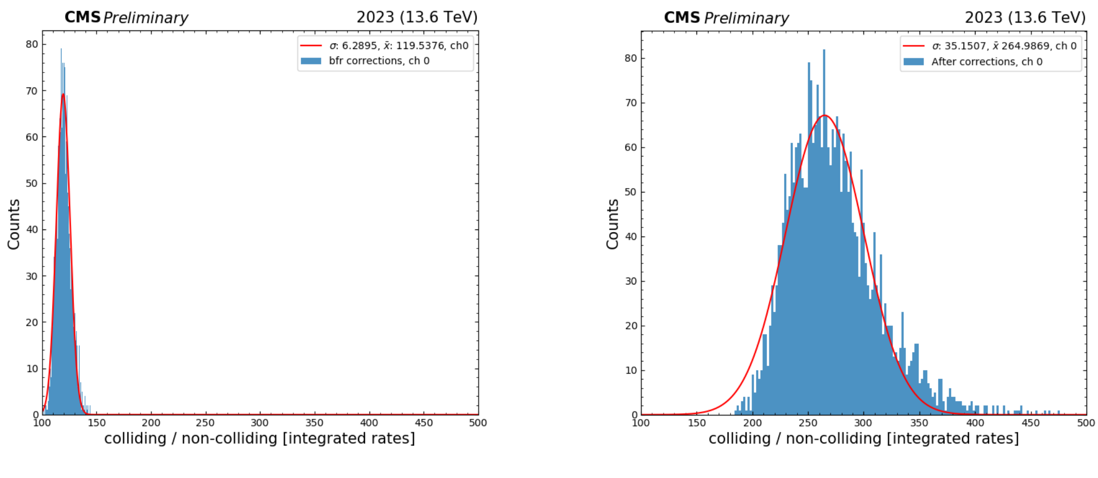

Figure 5.9: Figure (a) shows the distribution of the ratio of a colliding bcid to a non-colliding bcid before corrections. Figure (b) shows the result but after the corrections.

On the other hand, Figure 5.11 shows the number of counts for every

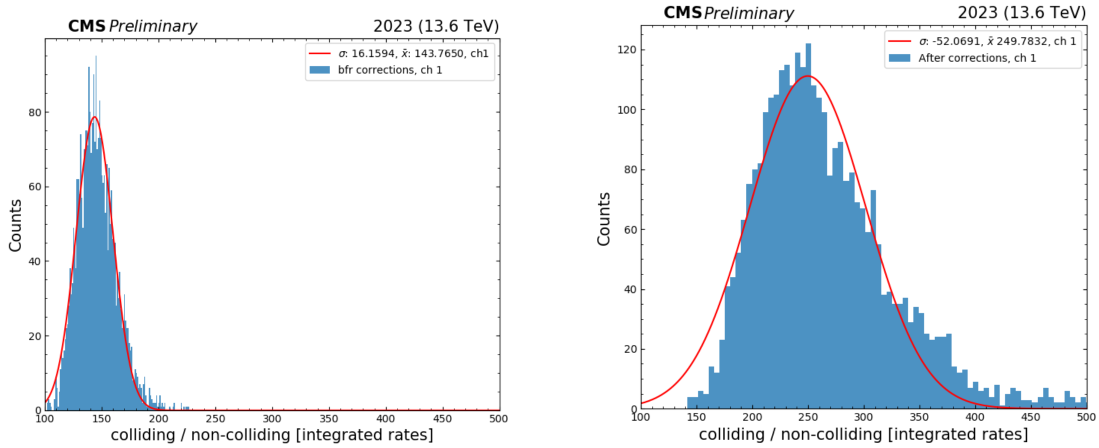

(a) (b)

Figure 5.10: Figure (a) shows the distribution of the ratio of a colliding bcid to a non-colliding bcid before corrections for channel 1. Figure (b) shows the result but after the corrections fot he same channel.

bcid so that one can compare the results after applying the corrections. Furthermore, in Figure 5.12 we can compare the integrated rates as a function of time for corrected and not corrected data.

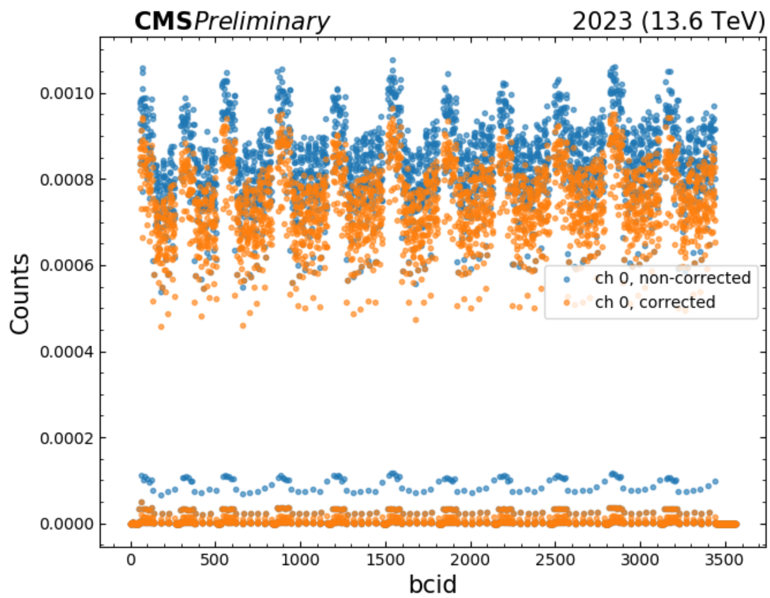

Figure 5.11: Type 1 afterglow hits corrections applied to every colliding bcid.

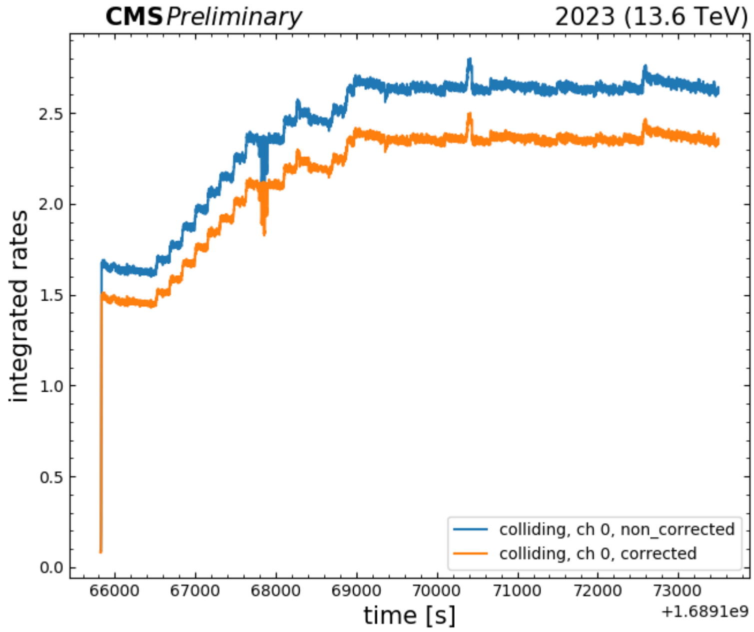

Figure 5.12: Type 1 afterglow hits corrections applied to every colliding bcid for channel 0.

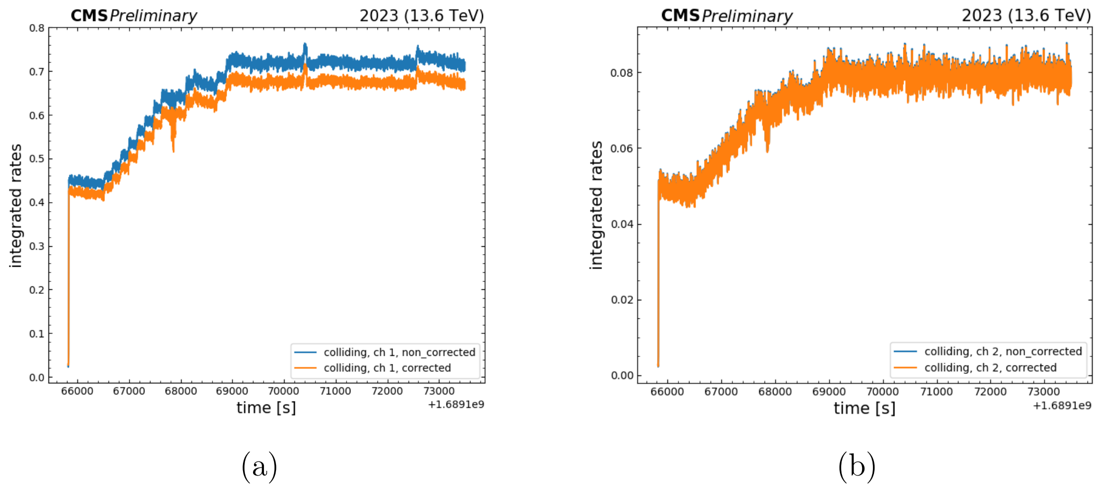

Figure 5.13: Figure (a) shows the integrated rates of colliding bcids before and after corrections for channel 1. Figure (b) shows the integrated rates of colliding bcids before and after corrections for channel 2.

Moreover, from channel 2 and above, as can be seen in figures 5.13 and 5.14 it gets difficult to see a difference between corrected and non-corrected data. This is because the location of the boards or channels provokes them to detect less rates. This is proved in Figure 5.15 in which we can see that, board 1 corresponds to a correction of $\approx 7.5\%$ and channels 2-4, after ap-

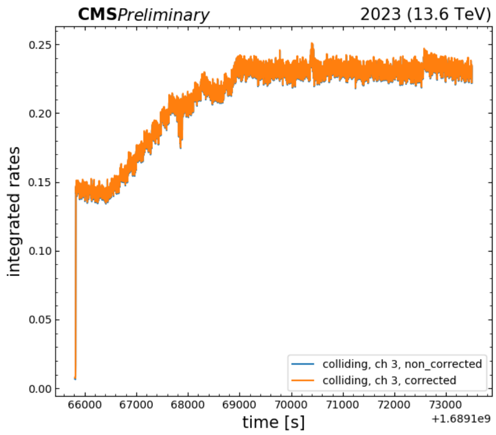

(a)

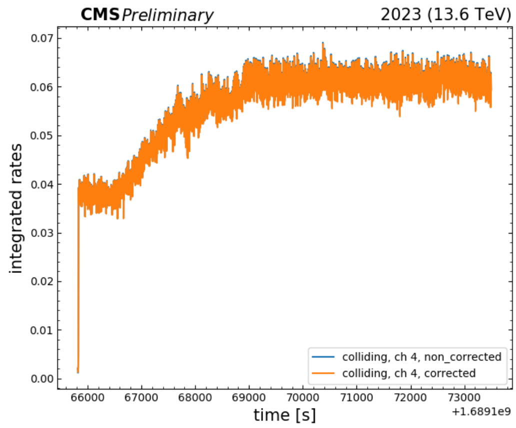

(b)

Figure 5.14: Figure (a) shows the integrated rates of colliding bcids before and after corrections for channel 3. Figure (b) shows the integrated rates of colliding bcids before and after corrections for channel 4.

plying corrections, the difference is negligible (between 0.001% and 2%).

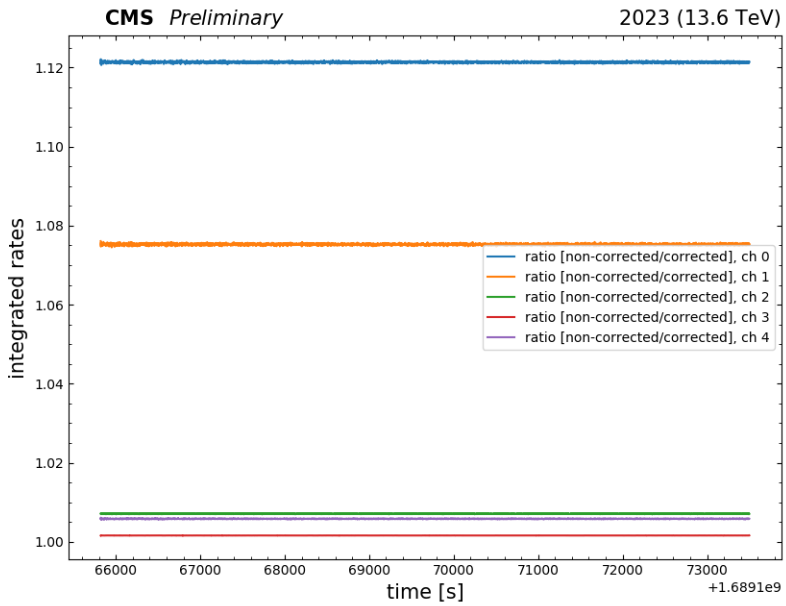

Figure 5.15: The ratio of non-corrected integrated rates to corrected integrate rates for all channels.

5.2 More background contributions

In this section, we study other types of backgrounds. These are beam induced and cosmic rays. For this purpose we compute the integrated rates separately for both, colliding bcids and non-colliding bcids. In addition, we also take into account some data that was recorded with no beam in the LHC.

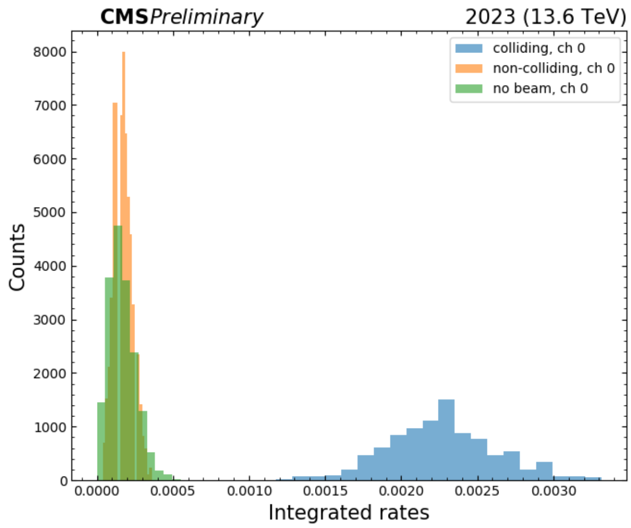

Figure 5.16: Integrated rates for colliding and non-colliding bcids for channel zero. In addition we have data recorded with no beam.

Figure 5.16 shows the distributions of the integrated rates for both types of data, the obtained with beam in the LHC and data obtained with no beam. One can see that the data of non-colliding bcids, overlaps the data with no beam. Since both shows agreement it is suitable to compute how much is the contribution of these backgrounds.

On the other hand, Figure 5.17, show that the mean value of beam induced background per bcid is $0.0022/3564 = 6.17\text{E-}7$ which is negligible compared to single bunch rate of 8E-4 (2400 bunches fill). However, it might have a significant impact on measured rates for the fills with a few bunches.

We took data during interfill to quantify the contribution from cosmics (and electronics noise). The rates were integrated over the orbit, the histogram shows variation of the multiple nb4 histograms. The results for channels 0 and 1 can be seen in Figure 5.18.

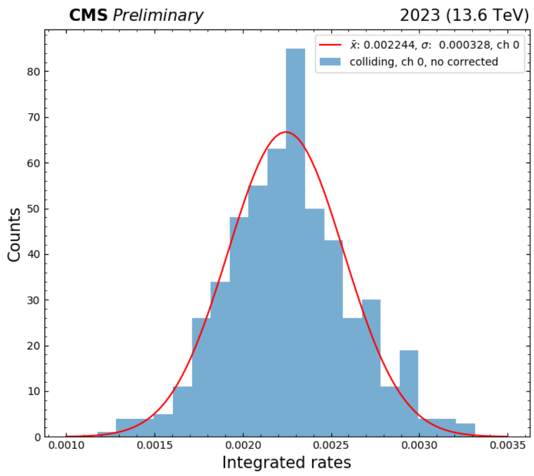

Figure 5.17: This figure shows the beam induced background for channel 0 including the fitting curve for estimating this contribution

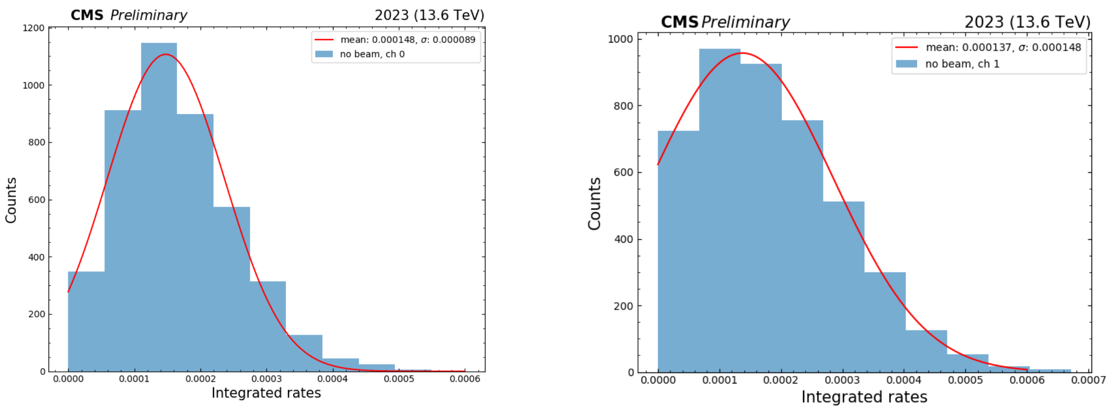

(a) (b)

Figure 5.18: Figure (a) shows the contributions of cosmics background for channel 0. Figure (b) shows the contributions of cosmics background for channel 1.

5.3 Luminosity Calibration

In this section we show the results of the luminosity calibration using data from fill 9062. The vdM framework (FW) was applied using a single gaussian SG. It can be seen, in Figure 5.20, that the computed xsec or sigma visible (σ_{vis}) is roughly 2.001μb. These results correspond to board 0. Moreover, there is a significant spread in the measured μb.

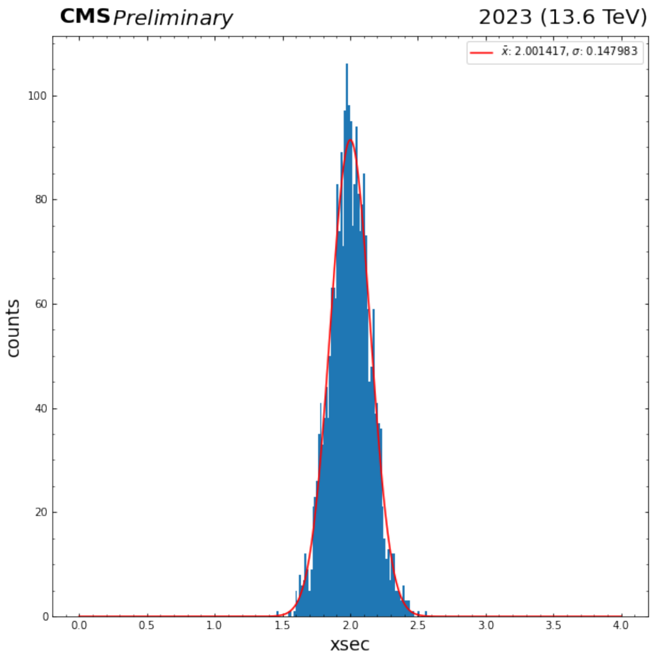

Figure 5.19: Data and fitting curve for channel 0.

Then, by using the following equation,

$$L = \frac{R \cdot f}{\sigma}$$

we can compute the instantaneous luminosity L. However, it is still needed to recalculate σ_{vis} after some corrections.

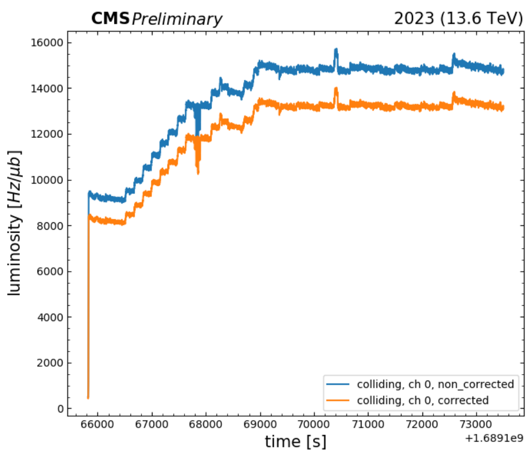

Figure 5.20: Luminosity for channel 0 after and before type1 afterglow corrections.

6 Conclusions

An analysis of background contributions such as type 1 afterglow hits, cosmics and beam induced was performed. The data acquisition was done by using a XDAQ application running on BRIL machine.

When looking at Figure 4.2 we still could see some non-zero rates in non-colliding bunch-crossings. This was attributed to cosmic background / electronics noise, out-of-time hits (Type1 afterglow). These contributions were quantified and could be added to XDAQ processor / offline processing routine.

After studying the backgrounds aforementioned, it was shown that the most important background is type 1 afterglow hits. However, the effect is less significant for channels above 1 since with limited rates it gets more difficult to correctly derive and suppress type 1. For example, board 0 and 1 correspond to a correction of $\approx 12\%$ and $\approx 7.5\%$ respectively, but for channels 2-4 the difference is negligible after applying corrections (between 0.01% and 2%).

Moreover, for cosmics and beam induced background we found that they are negligible. The mean value of beam induced background per bcid is $0.0022/3564 = 6.17E - 7$ which is negligible compared to single bunch rate of $8E - 4$. Beam induced background is 1000 times smaller.

Finally, a vdM framework was applied to data corresponding to fill 9062. Though the σ_{vis} has a error up to 14%, we could improve this measurement by applying corrections so that we can suppress outliers.

References

[1] G. P. M. Zanetti, “Study of the performance of the CMS Pixel Luminosity Telescope,” 2016.

[2] Peter Tsrunchev, “Luminosity measurements at CMS.”